DOI: 10.1534/genetics.109.110338

A Single Unpaired and Transcriptionally Silenced X Chromosome Locally Precludes Checkpoint Signaling in the *Caenorhabditis elegans* Germ Line

Aimee Jaramillo-Lambert and JoAnne Engebrecht[1]

Department of Molecular and Cellular Biology, Genetics Graduate Group, University of California, Davis, California 95616

Manuscript received September 28, 2009
Accepted for publication December 7, 2009

ABSTRACT

In many organisms, female and male meiosis display extensive sexual dimorphism in the temporal meiotic program, the number and location of recombination events, sex chromosome segregation, and checkpoint function. We show here that both meiotic prophase timing and germ-line apoptosis, one output of checkpoint signaling, are dictated by the sex of the germ line (oogenesis *vs.* spermatogenesis) in *Caenorhabditis elegans*. During oogenesis in feminized animals (*fem-3*), a single pair of asynapsed autosomes elicits a checkpoint response, yet an unpaired X chromosome fails to induce checkpoint activation. The single X in males and *fem-3* worms is a substrate for the meiotic recombination machinery and repair of the resulting double strand breaks appears to be delayed compared with worms carrying paired X chromosomes. Synaptonemal complex axial HORMA domain proteins, implicated in repair of meiotic double strand breaks (DSBs) and checkpoint function, are assembled and disassembled on the single X similarly to paired chromosomes, but the central region component, SYP-1, is not loaded on the X chromosome in males. In *fem-3* worms some X chromosomes achieve nonhomologous self-synapsis; however, germ cells with SYP-1-positive X chromosomes are not preferentially protected from apoptosis. Analyses of chromatin and X-linked gene expression indicate that a single X, unlike asynapsed X chromosomes or autosomes, maintains repressive chromatin marks and remains transcriptionally silenced and suggests that this state locally precludes checkpoint signaling.

In metazoans, sexual dimorphisms manifest not only striking morphological somatic forms but also distinct differences in female and male germ-line biology. In the germ line, meiosis is coupled to cellular differentiation programs that result in the production of two very distinct sex-specific haploid gamete types, oocytes and sperm. The regulation of meiosis can differ considerably between the sexes as reflected in both the phenotypic manifestations of mutants as well as the temporal program of events (Hunt and Hassold 2002; Morelli and Cohen 2005). For example, female mammals enter prophase *in utero* whereas males initiate prophase postnatally (Handel and Eppig 1998). In the nematode *Caenorhabditis elegans* prophase I for oogenesis in hermaphrodites (functionally female) takes twice as long as prophase I for spermatogenesis in males (Jaramillo-Lambert *et al.* 2007). Furthermore, female germ cells of many species initiate a meiotic arrest during prophase I that does not occur in male germ cells (Masui and Clarke 1979; Eppig *et al.* 1996; McCarter *et al.* 1999). In late meiotic prophase, chromosome morphology (Shakes *et al.* 2009), chromatin compaction (Wu and Chu 2008), and the presence of centriole-containing centrosomes (Manandhar *et al.* 2005; Shakes *et al.* 2009; Wignall and Villeneuve 2009) can also exhibit sex-specific differences.

With some exceptions, early events in meiotic prophase such as chromosome pairing and synapsis, the close alignment of homologous chromosomes through the elaboration of the synaptonemal complex (SC), are largely conserved between the sexes; however, the extent of genetic exchange can differ significantly. Meiotic recombination rates are higher in females compared to males in humans (Donis-Keller *et al.* 1987), mice (Blank *et al.* 1988), zebrafish (Singer *et al.* 2002), Drosophila (Morgan 1912), and *C. elegans* (Zetka and Rose 1990; Meneely *et al.* 2002). In virtually all of these organisms, however, sex not only affects the rate of recombination but also influences the placement of exchange events along the length of the chromosome. Too few, or inappropriately placed recombination events can lead to chromosome nondisjunction (Koehler *et al.* 1996; Lamb *et al.* 1996; Ross *et al.* 1996). In humans meiotic failure rates as measured by aneuploidy are higher in oocytes (up to 25%) than in sperm (2%) (Hassold and Hunt 2001). It has been proposed that checkpoints monitoring meiotic events such as recombination are less stringent in females compared to males. *C. elegans* also appears to have sex-

[1]*Corresponding author:* Department of Molecular and Cellular Biology, 1 Shields Ave., University of California, Davis, CA 95616.
E-mail: jengebrecht@ucdavis.edu

specific differences in checkpoint function; hermaphrodites respond to errors in synapsis, recombination, or DNA damage by culling germ cells through apoptosis (Gartner *et al.* 2000; Bhalla and Dernburg 2005; Stergiou *et al.* 2007). However, the male germ line does not induce apoptosis in response to DNA damage (Gartner *et al.* 2000).

The mechanism by which sex chromosomes (*e.g.*, XX female *vs.* XY male) segregate at meiosis I is of necessity different between the sexes. While the homogametic chromosome pair segregates similarly to autosomes, multiple strategies have evolved to segregate the heterogametic sex chromosomes. For example, in marsupial males, the X and Y chromosomes never synapse but remain associated through the formation of a dense plate (Page *et al.* 2006). In most male placental mammals the X and Y sex chromosomes pair, synapse, and undergo exchange at the small pseudoautosomal region, leaving the bulk of the sex chromosomes unpaired (Perry *et al.* 2001; Handel 2004). In a number of organisms, unpaired DNA in the germ line is transcriptionally silenced in a process referred to as meiotic silencing of unpaired chromatin (MSUC); meiotic sex chromosome inactivation (MSCI) of the unpaired regions of the X and Y has been proposed to be a related process and is important for completion of meiosis in male mice (Mahadevaiah *et al.* 2008). In chickens, the W and Z chromosomes of females achieve nonhomologous synapsis but still undergo MSCI, suggesting that transcriptional silencing is important for the heterogametic sex regardless if male or female (Schoenmakers *et al.* 2009).

Double strand breaks (DSBs) and their repair via the homologous chromosome are essential for chromosome segregation during the first meiotic division (Kleckner 1996; Roeder 1997; Zickler and Kleckner 1999). Surprisingly, asynapsed regions of the mammalian XY bivalent incur DSBs (Ashley *et al.* 1995; Moens *et al.* 1997), yet lack a homologous chromosome for repair and must use the sister chromatid as template, a situation that normally triggers a checkpoint response. An outstanding question remains, namely, what prevents constitutive checkpoint activation in the germ line of the heterogametic sex?

Here, we analyzed several aspects of female and male meiosis in the *C. elegans* germ line. *C. elegans* exists predominantly as a self-fertilizing hermaphrodite; during development, hermaphrodites initially produce sperm and then switch to making oocytes, and thus as adults are female. However, males arise spontaneously in the population at a low frequency due to meiotic chromosome nondisjunction and can be maintained through genetic crosses. *C. elegans* has six chromosomes: five autosomes and one sex chromosome, the X. The ratio of the number of X chromosomes to the number of autosomes determines sex (XX/AA = 1 is hermaphrodite; X0/AA = 0.5 is male) (Madl and Herman 1979). We show that meiotic prophase kinetics and germ-line apoptosis are controlled in a sex-specific manner in *C. elegans*. Taking advantage of the availability of sex determination mutants, we discovered that a single X has unique properties that prevent the checkpoint machinery from recognizing the X as asynapsed. We also found that a single X chromosome incurs meiotic DSBs, and repair of these breaks appears to be delayed. SC axial components that play roles in interhomolog bias during meiotic recombination and checkpoint signaling are assembled on the single X, indicating that failure in checkpoint activation is not due to the absence of these proteins. Our studies suggest that detection of asynapsis by checkpoints is regulated by the chromatin/transcriptional status of the chromosome.

MATERIALS AND METHODS

Genetics: Except where noted all *C. elegans* strains (Bristol N2 background) were propagated under standard procedures at 20° (Brenner 1974). The following strains were used: CB2754: *tra-2(e1095)/dpy-10(e128) unc-4(e120)* II; JK816: *fem-3(q20)* IV; JK551: *unc-5(e53) fem-3(q22)* IV; JK2878: *fog-1(q325)* I/*hT2* (I;III); CB1489: *him-8(e1489)* IV; CA151: *him-8(me4)* IV; CB678 *lon-2(e678)* X; AV106: *spo-11(ok79)* IV/*nT1* (IV;V); *fem-3(e1996)/nT1-GFP* IV (a generous gift from Tim Schedl), and CA258: *zim-2(tm574)* IV. Some nematode strains used in this work were provided by the Caenorhabditis Genetics Center, which is funded by the National Institutes of Health National Center for Research Resources (NCRR).

To generate homozygous *fem-3(e1996) X0* animals, homozygous *fem-3(e1996); lon-2(e678) XX* females were mated to *fem-3(e1996)/nT1-GFP X0* males and nongreen, long animals were selected for analysis. To generate homozygous *fog-1(q325) X0* worms, *fog-1(q325)/hT2-GFP XX* hermaphrodites were crossed to N2 *X0* males. Nongreen male cross progeny were then mated to homozygous *fog-1(q325) XX* females and the male cross progeny carrying oocytes were selected. *tra-2(e1095)* was maintained over *dpy-10 unc-4(e120)* alleles by picking heterozygous hermaphrodites (wild-type phenotype). Homozygous *tra-2(e1095) XX* males were a product of the heterozygous self-mating. To elicit the temperature-sensitive phenotype of *fem-3(q20)* and *fem-3(q22)*, L3 progeny were shifted to 25° 26 hr prior to injection or 48 hr prior to examining germ lines for apoptosis (this early shift to 25° prevents the formation of any oocytes).

Meiotic prophase progression kinetics: Microinjection of Cy3-dUTP (Amersham Biosciences; Piscataway, NJ) and meiotic progression assays were carried out as in (Jaramillo-Lambert *et al.* 2007).

RNA interference: RNAi was performed by the feeding method of (Timmons *et al.* 2001). L4 worms [L3 for the *fem-3(q22)* strain] were fed bacteria expressing double stranded RNA to indicated gene (*syp-1*, *him-8*, *zim-1*, *zim-2*, *pch-2*, and *chk-1*) from RNAi feeding library (Kamath *et al.* 2003). RNAi efficacy was monitored by counting DAPI staining bodies in hermaphrodite diakinesis nuclei (*him-8*, *zim-1*, and *zim-2*) and by monitoring plates for dead embryos and incidence of male progeny (*syp-1*). *chk-1(RNAi)* efficiency was determined by monitoring progeny for sterility. Bacteria expressing feeding vector (L4440) were used as controls. Cells were seeded onto NGM plates that contained 25 μg/ml carbenicillin

and 1 mM IPTG and allowed to grow at room temperature for 24 hr. Seeded plates were stored at 4° and used within ~2 weeks.

Quantification of germ-line apoptosis: Acridine orange (AO) staining of apoptotic germ cells in *tra-2(e1095) XX*, *fog-1(q325) X0*, *fem-3(e1996) X0*, N2 *XX*, and N2 *X0* was carried out using modifications of procedure in (Gartner *et al.* 2004). *tra-2(e1095) XX* and wild-type control animals were synchronized by picking L4 larvae to new plates and holding at 20° for 48 hr. *fog-1(q325) X0, fem-3(e1996) X0*, and wild-type controls were synchronized by picking L4 larvae to fresh plates and incubating at 20° for 24 hr. A total of 0.5 ml of 50 μg/ml AO (Molecular Probes, Invitrogen; Carlsbad, CA) in M9 was added to 60-mm plates containing adult worms and incubated at room temperature for 1 hr. Worms were replated to new 60-mm plates, allowed to recover, and then mounted under cover slips in M9 on 3% agarose pads containing 0.2 mM tetramisole (Sigma; St. Louis). Apoptotic bodies were scored by fluorescence microscopy and DIC.

fem-3(q22) XX and wild-type controls were synchronized by picking L3 larvae and holding at either the permissive (15°) or restrictive (25°) temperatures for 48 hr. Apoptosis was scored by CED-1-GFP fluorescence (Bhalla and Dernburg 2005); CED-1 is a transmembrane protein on phagocytic cells that is important for engulfment of apoptotic cells (Zhou *et al.* 2001).

Germ-line apoptosis in N2 *XX* hermaphrodites and *fem-3(e1996) X0* animals subjected to RNAi was quantified by CED-1-GFP 48 hr post-L4 larvae.

Immunostaining: Rabbit anti-RAD-51 (1:50) (Colaiácovo *et al.* 2003), rabbit anti-SYP-1 (1:200), and guinea pig anti-SYP-1 (1:800) (MacQueen *et al.* 2002) were generous gifts from A. Villeneuve. Guinea pig anti-HIM-8 (1:500) (Phillips *et al.* 2005), guinea pig anti-HTP-3 (1:500) (MacQueen *et al.* 2005), and rabbit anti-HTP-1/2 (1:500) (Martinez-Perez *et al.* 2008) were generously donated by A. Dernburg. Rabbit anti-HIM-3 (1:200) (Zetka *et al.* 1999) was generously provided by M. Zetka. Rabbit anti-GFP (1:500) was purchased from Novus Biologicals (Littleton, CO). Rabbit anti-histone H3 dimethyl-lysine 9 (H3dimethylK9) (1:500) (Kelly *et al.* 2002) was purchased from Upstate USA (Charlottesville, VA). Rabbit anti-histone H3 dimethyl-lysine 4 (H3dimethylK4) (1:500) (Kelly *et al.* 2002) was purchased from Cell Signaling Technology (Danvers, MA). The secondary antibodies Alexa Fluor-488 donkey anti-rabbit (1:200), Alexa Fluor-555 donkey anti-rabbit (1:200), and Alexa Fluor-488 goat anti-guinea pig (1:200) were purchased from Molecular Probes, Invitrogen. Antibody staining of gonads was performed as in Jaramillo-Lambert *et al.* (2007). The slides were imaged using an API Delta Vision deconvolution microscope. Images were deconvolved using Applied Precision SoftWoRx image analysis software.

RAD-51 foci were quantified in three germ lines of age-matched hermaphrodites and males (20 hr post-L4) of each genotype (Colaiácovo *et al.* 2003). Germ lines were divided by meiotic prophase substage and number of foci per nucleus was scored for each stage. Quantification of RAD-51 foci specific to the X chromosome(s) was scored as foci that localized to the chromosome that stained with the X-specific marker, HIM-8. Data were analyzed using Applied Precision SoftWoRx image analysis deconvolution software.

RNA *in situ* hybridization: Gonads were dissected and processed on slides as described for batch processing (Lee and Schedl 2006). Both sense and antisense probes were synthesized for the X-linked, oocyte-enriched genes, K08A8.1 and F52D2.2 (Reinke *et al.* 2000; Kelly *et al.* 2002). The control sense probes gave little or no signal (data not shown). Images were captured with a Zeiss Axioplan 2 microscope equipped with a color Axiocam.

RESULTS

Meiotic prophase progression is dependent on the sex of the germ line: The *C. elegans* germ line is housed in two (hermaphrodites) or one (male) U-shaped gonads; syncytial germ cells within the gonad are arranged in a temporal/spatial gradient with classical stages of meiotic prophase easily distinguishable (Figure 1A) (Hubbard and Greenstein 2005). We previously developed an S phase labeling assay and found that meiotic prophase progression for oogenesis in adult hermaphrodites takes twice as long as meiotic prophase progression for spermatogenesis in adult males (54–60 hr *vs.* 20–24 hr) (Jaramillo-Lambert *et al.* 2007). To determine whether the difference in timing is dependent on chromosome sex (XX *vs.* X0), somatic sex (female *vs.* male body), or germ-line sex (oogenesis *vs.* spermatogenesis) we used S phase labeling (Jaramillo-Lambert *et al.* 2007) to monitor progression of nuclei through the meiotic prophase substages over time in several sex determination mutants that uncoupled chromosome, somatic, and germ-line sex.

fem-3(e1996lf) X0 animals have a female body and undergo oogenesis (Hodgkin 1986), while *fog-1(q325lf) X0* animals have a male body, but an oogenic germ line (Barton and Kimble 1990). Meiotic prophase timing in these mutants was slow (54–60 hr), similar to N2 *XX* hermaphrodites. Progression of labeled nuclei through each prophase substage in *fem-3(lf) X0* and *fog-1(lf) X0* similarly paralleled N2 *XX* hermaphrodites (Figure 1B). These experiments reveal that irrespective of the number of X chromosomes or whether there is a male or female body, mutants undergoing oogenesis have slow meiotic prophase kinetics.

We also examined prophase kinetics of *tra-2(e1095lf) XX* and *fem-3(q20gf) XX* mutants. *tra-2(lf) XX* animals have a male body and spermatogenic germ line (Hodgkin and Brenner 1977). Prophase progression timing of *tra-2(lf) XX* males was similar to N2 *X0* males with prophase completed by 20–24 hr; progression of nuclei through each substage was similar to N2 *X0* males, although there were fewer labeled nuclei in the transition zone in *tra-2(lf) XX* compared to N2 *X0* males (Figure 1C). *fem-3(q20gf) XX* animals have a female soma, but the germ line only produces sperm at 25°, the nonpermissive temperature (Barton *et al.* 1987). Analysis of meiotic prophase progression in N2 *X0* males revealed that prophase took slightly less time at 25° compared to standard temperature of 20° (completed between 16–21 hr; Figure 1C). Similarly, meiotic prophase kinetics of *fem-3(gf) XX* animals (25°) was completed by 21 hr (Figure 1C). Thus, worms undergoing spermatogenesis have fast meiotic prophase kinetics. Taken together, these results indicate that meiotic prophase timing is dictated by the sex of the germ line.

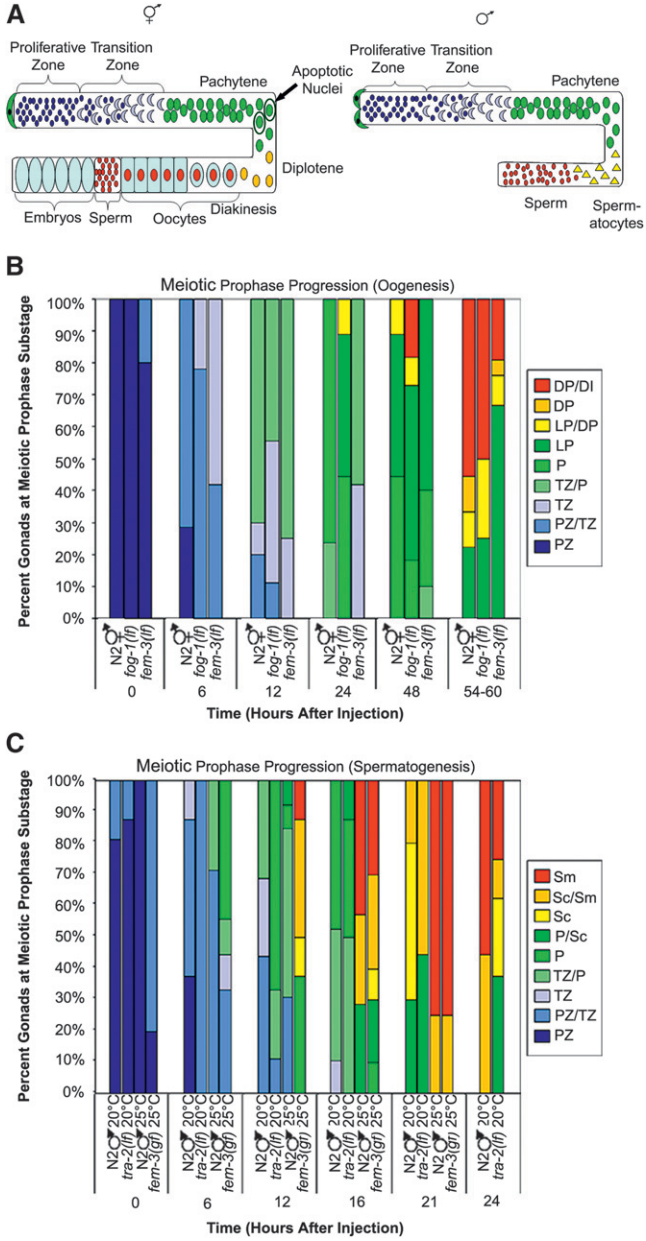

FIGURE 1.—Meiotic prophase progression is dependent on germ-line sex. (A) Cartoon of hermaphrodite (left) and male (right) gonad arms. Distal end is capped by somatic distal tip cell(s) (green) and contains a population of proliferating germ cells (dark blue). As cells move proximally they enter meiotic prophase (transition zone-leptotene/zygotene; light blue crescents) and then progress through pachytene (green), diplotene (yellow), and diakinesis (red). Initially, hermaphrodites form sperm (small red circles) and then switch to oocyte production (light blue with red centers) beginning at L4 stage. After switch to oocyte production, cells in the pachytene region of the germ line undergo physiological apoptosis (circled green nuclei). In males, germ-line cells differentiate into spermactocytes (yellow triangles) and then sperm (red circles); no apoptosis occurs. (B) Meiotic prophase timing in sex determination mutants undergoing oogenesis. Percentage of gonads displaying labeled nuclei at indicated stages is shown. Proliferative zone (PZ), transition zone (TZ), pachytene (P), late pachytene (LP), diplotene (DP), and diakinesis (DI). Number of gonads examined at each time point were N2 *XX*: 0 hr = 9, 6 hr = 14, 12 hr = 10, 24 hr = 17, 48 hr = 9, and 54–60 hr = 9; *fog-1(q325) X0*: 0 hr = 7, 6 hr = 9, 12 hr = 9, 24 hr = 9, 48 hr = 11, and 54–60 hr = 8; and *fem-3(e1996) X0*: 0 hr = 10, 6 hr = 12, 12 hr = 8, 24 hr = 12, 48 hr = 10, and 54–60 hr = 18. (C) Meiotic prophase timing in sex determination mutants undergoing spermatogenesis. Percentage of gonads with labeled nuclei at indicated stages is shown. Proliferative zone (PZ), transition zone (TZ), pachytene (P), spermatocytes (Sc), and sperm (Sm). Number of gonads examined at each time point were N2 *X0* 20°: 0 hr = 16, 6 hr = 8, 12 hr = 16, 16 hr = 19, 21 hr = 10, and 24 hr = 9; *tra-2(e1095) XX* 20°: 0 hr = 8, 6 hr = 8, 12 hr = 9, 16 hr = 8, 21 hr = 9, and 24 hr = 8; N2 X0 25°: 0 hr = 7, 6 hr = 7, 12 hr = 13, 16 hr = 7, and 21 hr = 4 (15/19 gonads no label); and *fem-3(q20) XX* 25°: 0 hr = 10, 6 hr = 9, 12 hr = 8, 16 hr = 10, and 21 hr = 8.

Physiological and checkpoint-activated germ-line apoptosis are dependent on germ-line sex: Another striking germ-line difference between hermaphrodites and males is apoptosis. Nuclei in the pachytene region of the hermaphrodite germ line undergo both physiological and checkpoint-activated apoptosis (Figure 1A) (GUMIENNY *et al.* 1999; GARTNER *et al.* 2000; BHALLA and DERNBURG 2005). Contrastingly, the male germ line does not undergo physiological apoptosis (GUMIENNY *et al.* 1999) or apoptosis in response to exogenous DNA damage (GARTNER *et al.* 2000). To determine whether nuclei in the male germ line undergo checkpoint-activated apoptosis in response to chromosome asynapsis, and/or failure to repair meiotic DSBs, we examined apoptosis in germ lines where *syp-1* was depleted by RNAi. SYP-1 is a central region component of the SC; knockdown of *syp-1* results in increased levels of germline apoptosis in hermaphrodites because all chromosome pairs are asynapsed and chiasmata are not formed (Figure 2A) (MACQUEEN *et al.* 2002). In contrast to hermaphrodites, no apoptosis was observed in the male germ line when chromosome asynapsis was induced by depletion of *syp-1* (Figure 2B).

To determine whether checkpoint-activated apoptosis is under the same genetic control as meiotic prophase progression, we examined the sex determination mutants analyzed above (Figure 1) for both physiological (L4440; feeding vector) and checkpoint-activated apoptosis [*syp-1(RNAi)*]. Apoptosis in oogenic germ lines was quantified for N2 *XX*, *fem-3(lf) X0*, and *fog-1(lf) X0* using the vital dye, AO. Both *fem-3(lf) X0* and *fog-1(lf) X0* germ lines are competent for physiological apoptosis as shown by the low levels of apoptotic bodies seen in control worms (Figure 2A). This is consistent with previous analysis that indicated that oogenesis dictates physiological apoptosis (GUMIENNY *et al.* 1999). Additionally, when SYP-1 was depleted, both *fem-3(lf) X0* and *fog-1(lf) X0* worms had increased levels of apoptosis (Figure 2A). Thus oogenic germ lines undergo both physiological and checkpoint-activated apoptosis.

Apoptosis in N2 *X0* males, *tra-2/dpyunc XX* hermaphrodites, and *tra-2/tra-2 XX* mutants was also quantified

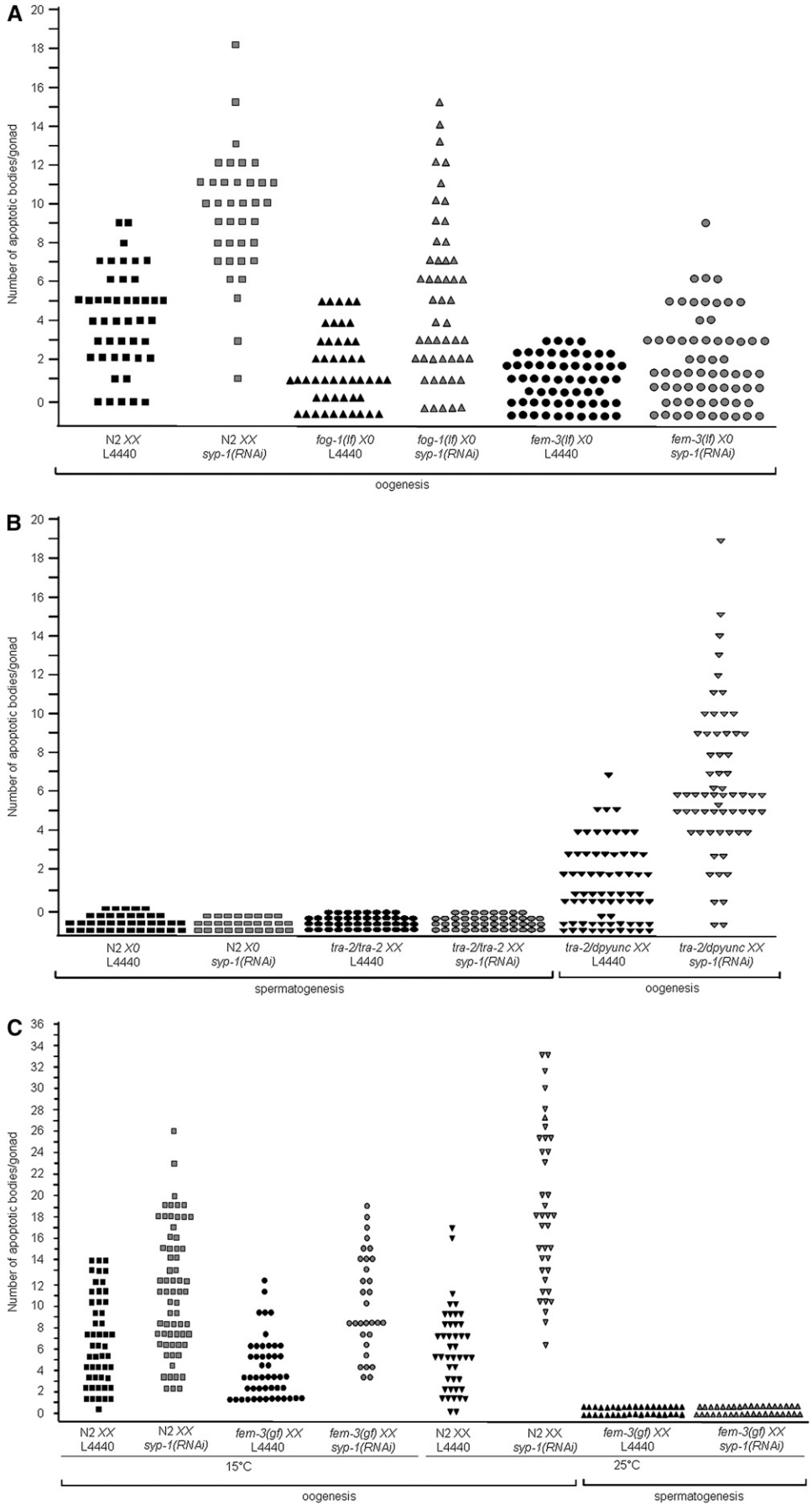

FIGURE 2.—Physiological and checkpoint-activated apoptosis are dependent on germ-line sex. (A) Scatterplot depicting number of apoptotic bodies detected in germ lines of N2 *XX*, *fog-1(q325) X0*, and *fem-3(e1996) X0* animals (by AO staining and DIC). Apoptosis was scored in adult animals 24 hr post-L4. *Y*-axis value for each point represents number of apoptotic bodies/gonad. Total number of gonads examined for each: N2 *XX* L4440 $N = 50$, N2 *XX syp-1(RNAi)* $N = 52$, *fog-1(q325) X0* L4440 $N = 48$, *fog-1(q325) X0 syp-1(RNAi)* $N = 50$, *fem-3(e1996) X0* L4440 $N = 60$, and *fem-3(e1996) X0 syp-1(RNAi)* $N = 66$. (B) Scatterplot depicting number of apoptotic bodies detected in germ lines of N2 *X0*, *tra-2 XX*, or *tra-2/dpyunc XX* worms (by AO staining and DIC). Apoptosis was scored in adult animals 48 hr post-L4. *Y*-axis value for each point represents number of apoptotic bodies/gonad. Total number of gonads examined for each: N2 *X0* L4440 $N = 37$, N2 X0 *syp-1(RNAi)* $N = 28$, *tra-2(e1095) XX* L4440 $N = 44$, *tra-2(e1095) XX syp-1(RNAi)* $N = 44$, *tra-2(e1095)/dpyunc XX* L4440 $N = 70$, and *tra-2(e1095)/dpyunc XX syp-1(RNAi)* $N = 57$. (C) Scatterplot depicting number of apoptotic bodies detected in gonads of N2 *XX* and *fem-3(q22) XX* worms by CED-1::GFP fluorescence, for both control (L4440) and *syp-1(RNAi)*. *fem-3(q22)* is temperature sensitive and each experiment was performed at both 15° and 25°. Apoptotic bodies were scored in adult animals 48 hr post-L3. *Y*-axis values represent number of apoptotic bodies/gonad. Total number of gonads examined for 15°: N2 *XX* L4440 $N = 50$, N2 *XX syp-1(RNAi)* $N = 65$, *fem-3(q22) XX* L4440 $N = 48$, and *fem-3(q22) XX syp-1(RNAi)* $N = 31$. Total number of gonads examined for 25°: N2 *XX* L4440 $N = 44$, *fem-3(q22) X0* L4440 $N = 36$, N2 *XX syp-1(RNAi)* $N = 38$, and *fem-3(q22) XX syp-1(RNAi)* $N = 37$.

using AO. *tra-2/dypunc XX* hermaphrodites were competent for both physiological and checkpoint-activated apoptosis, but no apoptosis was observed in N2 *X0* and *tra-2/tra-2 XX* males under either condition (Figure 2B). Apoptosis in N2 *XX* hermaphrodites and the *fem-3(gf) XX* mutant was scored at both the permissive (15°) and restrictive (25°) temperature by CED-1-GFP fluorescence (Boulton *et al.* 2004; Bhalla and Dernburg 2005). At 15° germ-line differentiation of *fem-3(gf) XX* behaves like N2 *XX*, first undergoing spermatogenesis and then switching to oogenesis as an adult. N2 *XX* and *fem-3(gf) XX* at 15° were competent for both physiological and checkpoint-activated apoptosis (Figure 2C). However, at 25° *fem-3(gf) XX* germ cells in the adult continued spermatogenesis and were not competent for either physiological or checkpoint-activated apoptosis (Figure 2C). Together these experiments indicate that regardless of X chromosome content or somatic sex, both physiological and checkpoint-activated apoptosis are dictated by the sex of the germ line.

The single X chromosome is not recognized to be partnerless: Checkpoints operate in meiosis to monitor both the status of chromosome synapsis and meiotic DSB repair and can detect a single asynapsed chromosome pair (Bhalla and Dernburg 2005; Hochwagen and Amon 2006). Analysis of apoptosis in *fem-3(lf) X0* and *fog-1(lf) X0* germ lines revealed low levels of basal apoptosis (Figure 2A, L4440), even though they have an asynapsed X. To confirm that checkpoints were not activated in *fem-3(lf) X0* worms, we monitored apoptosis in *fem-3(lf) X0* worms depleted for either *chk-1* or *pch-2*. CHK-1 is a conserved checkpoint kinase that functions in both the DNA damage and recombination checkpoint to activate p53 for apoptosis (Walworth and Bernards 1996; Levine 1997; Harrison and Haber 2006); PCH-2 is a AAA-ATPase that has been implicated in the chromosome synapsis checkpoint in *C. elegans* (Bhalla and Dernburg 2005), although the pathway and interaction with the recombination checkpoint has not been elucidated. Consistent with the absence of checkpoint activation, we observed no decrease in apoptosis when *chk-1* or *pch-2* was depleted in *fem-3(lf) X0* (Table 1), suggesting that neither the recombination nor synapsis checkpoint pathways are induced in *fem-3(lf) X0* animals.

To determine whether failure to recognize the asynapsed X chromosome is a unique property of the X or due to the inability to detect low levels of checkpoint signaling, we examined the consequence of inducing asynapsis of different autosomal pairs in *fem-3(lf) X0* worms. We observed increased levels of apoptosis in both N2 *XX* and *fem-3(lf) X0* worms when asynapsis of a single autosome pair (Phillips and Dernburg 2006), two autosome pairs (Phillips and Dernburg 2006), or all chromosome pairs were induced (MacQueen *et al.* 2002) (Table 1). Further, the increase in apoptosis in *syp-1(RNAi)* worms was dependent on both *chk-1* and *pch-2* (Table 1). On the other hand, depletion of *him-8*, which is important for X chromosome pairing and synapsis (Phillips *et al.* 2005), resulted in increased levels of apoptosis in N2 *XX* but not *fem-3(lf) X0* worms (Table 1). These results suggest that the lone X escapes detection by the checkpoint machinery.

TABLE 1

***fem-3(lf) X0* germ lines sense a single pair of asynapsed autosomes but not the unpaired X chromosome**

RNAi	Asynapsed chromosomes	No. apoptotic bodies/gonads	
		N2 *XX*	*fem-3(lf) X0*
L4440	NA	5.6 ± 0.3	1.8 ± 0.2
zim-2	V	8.2 ± 0.6*	4.9 ± 0.6*
zim-1	II and III	12.0 ± 1.5*	3.9 ± 0.5*
syp-1	All	14.0 ± 0.8*	5.2 ± 0.5*
chk-1	NA	5.1 ± 0.8	1.8 ± 0.7
syp-1;chk-1	All	4.6 ± 0.8	2.8 ± 0.7
pch-2	NA	7.5 ± 1.0	1.5 ± 0.3
syp-1;pch-2	All	9.1 ± 1.9*	2.4 ± 0.4
him-8	X	9.9 ± 1.1*	2.4 ± 0.3

Number of apoptotic nuclei/gonad arm was determined by CED-1-GFP 48 hr post-L4. Minimum of 15 gonad arms were scored for each genotype. Average number of bivalents/univalents in diakinesis oocytes by DAPI staining for L4440 = 5.7, *zim-2(RNAi)* = 6.5, *fem-3(e1996); zim-2(RNAi)* = 6.4, *zim-1(RNAi)* = 7.0, *fem-3(e1996); zim-1(RNAi)* = 7.4, and *him-8(RNAi)* = 6.4. *syp-1(RNAi)* efficiency was determined by monitoring plates for dead embryos and male progeny. The data shown are means ± SEM Statistical comparisons between the mutants and L4440 were conducted using the two-tailed Mann-Whitney test. *$P < 0.001$.

Double strand break levels are elevated and perdure in X0 animals: During meiosis the intentional formation of DSBs, and repair via the homologous chromosome, is needed to form chiasmata essential for chromosome segregation at the first meiotic division (Lee and Amon 2001). In hermaphrodites, failure in chromosome synapsis activates the recombination checkpoint pathway leading to increased levels of apoptosis due to the absence of a homologous partner for repair of DSBs (MacQueen *et al.* 2002; Colaiácovo *et al.* 2003; Smolikov *et al.* 2007, 2009). As the male X chromosome has no homologous chromosome to repair DSBs and fails to activate the apoptotic pathway even in an oogenic germ line [*fem-3(lf) X0*, Figure 2A, Table 1], we reasoned that the single X chromosome does not incur DSBs. To examine DSBs specifically on the X chromosome(s) in germ-line nuclei of wild-type and mutant animals we monitored the localization of the strand exchange protein RAD-51, which is transiently associated with DSBs (Alpi *et al.* 2003), as well as HIM-8, an X-specific transacting factor (Phillips *et al.* 2005) (Figure 3A). In germ lines of N2 *XX* hermaphrodites and *tra-2 XX* male mutants the majority of nuclei did not have RAD-51 foci on the X chromosome pair at the time of dissection, but 15 and 13% of early and 7 and

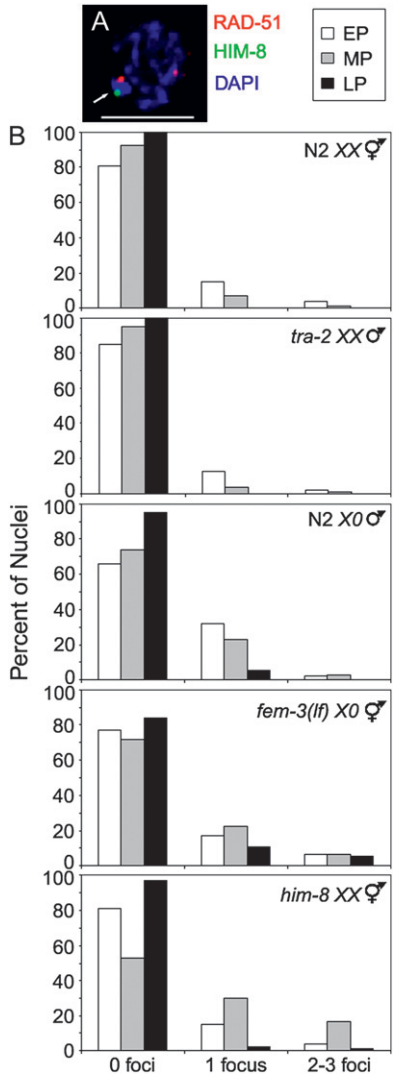

Figure 3.—Abundance of RAD-51 foci on X chromosome(s). (A) Nucleus showing RAD-51 focus on X (arrow). Nucleus labeled with α-RAD-51 (red) and α-HIM-8 (green), counterstained with DAPI (blue). Scale bar, 5 μm. (B) Histograms representing quantification of RAD-51 foci on X chromosome(s) in N2 *XX*, *tra-2 XX* males, N2 *X0*, *fem-3(e1996) X0*, and *him-8(me4) XX*. *Y*-axis indicates percentage of nuclei that contain 0, 1, or 2–3 RAD-51 foci per X chromosome for early pachytene (white), midpachytene (gray), and late pachytene (black).

4% of midpachytene nuclei, respectively, had one RAD-51 focus, and <5% had two to three RAD-51 foci. By late pachytene there were no RAD-51 foci detected on the X chromosome pair in these germ lines (Figure 3B, top two histograms). In contrast, 32% of early pachytene and 23% of midpachytene nuclei of N2 *X0* male germ lines had one focus while 2% in early and 3% in midpachytene had two to three RAD-51 foci. In *fem-3(lf) X0* mutant germ lines 17% in early pachytene and 22% in midpachytene had one RAD-51 focus on the X chromosome while 6% in both early and midpachytene had two to three RAD-51 foci. In both N2 *X0* male and *fem-3(lf) X0* germ lines RAD-51 foci were also detected in late pachytene nuclei (Figure 3B, middle two histograms). The overall increase in the number of Xs with RAD-51 foci was similar to what was observed in *him-8(me4) XX* germ lines where RAD-51 foci were elevated on the asynapsed X chromosomes and persisted into late pachytene (Figure 3B, bottom histogram). This analysis was possible as the *him-8(me4)* is a missense mutation that encodes a protein that binds the X chromosome and is still recognized by HIM-8 antibodies (Phillips *et al.* 2005). The RAD-51 foci observed on the single X in N2 males were SPO-11 dependent, indicating that breaks were induced by the meiotic recombination machinery (data not shown). Taken together, these data indicate that the single X chromosome is a substrate for the meiotic recombination machinery and suggest that the dynamics of DSB repair on the X chromosome(s) is influenced by the lack of a homologous chromosome.

In mutant hermaphrodite germ lines that are unable to repair breaks due to unavailability of the homologous chromosome there is an apparent global increase in the number of DSBs as well as a persistence of breaks on all chromosomes into late stages of pachytene (Colaiácovo *et al.* 2003; Carlton *et al.* 2006; Smolikov *et al.* 2007, 2009). To determine whether DSBs on the single X chromosome in N2 males also had this effect, we examined the global appearance and removal of RAD-51 in male and hermaphrodite germ lines. RAD-51 foci in N2 *XX* germ lines appeared in the transition zone, peaked during early pachytene, and disappeared by late pachytene (Figure 4B) (Colaiácovo *et al.* 2003; Carlton *et al.* 2006). RAD-51 foci in N2 *X0* male germ lines also first appeared in the transition zone, but quantification revealed higher overall levels of RAD-51 foci and a persistence of these foci into the late pachytene substage of meiotic prophase (Figure 4, A and B).

Progression of RAD-51 focus formation was also examined in *tra-2 XX* male and *fem-3(lf) X0* female germ lines. In *tra-2 XX* mutant germ lines, RAD-51 foci progression and abundance mirrored N2 *XX* hermaphrodite germ lines (Figure 4B). In *fem-3(lf) X0* germ lines, the progression of RAD-51 focus formation and removal was similar to N2 *X0* males where RAD-51 foci were shifted to later meiotic prophase substages and overall levels were higher (Figure 4B). This resembled what was observed in *him-8(me4) XX* hermaphrodite germ lines (Figure 4B, bottom), where asynapsis of a single chromosome pair has global effects on RAD-51 progression (Carlton *et al.* 2006). We also observed an extension of the transition zone in N2 *X0* and *fem-3(lf) X0* germ lines compared to *tra-2 XX* male and N2 *XX* hermaphrodite germ lines, respectively, as in *him-8 XX* hermaphrodite germ lines (data not shown; Figure 1, B and C; Carlton *et al.* 2006). Thus, the single X chromosome of males and *fem-3(lf)* mutants has global effects on DSB repair and meiotic prophase progression in the germ line; however, this does not result in

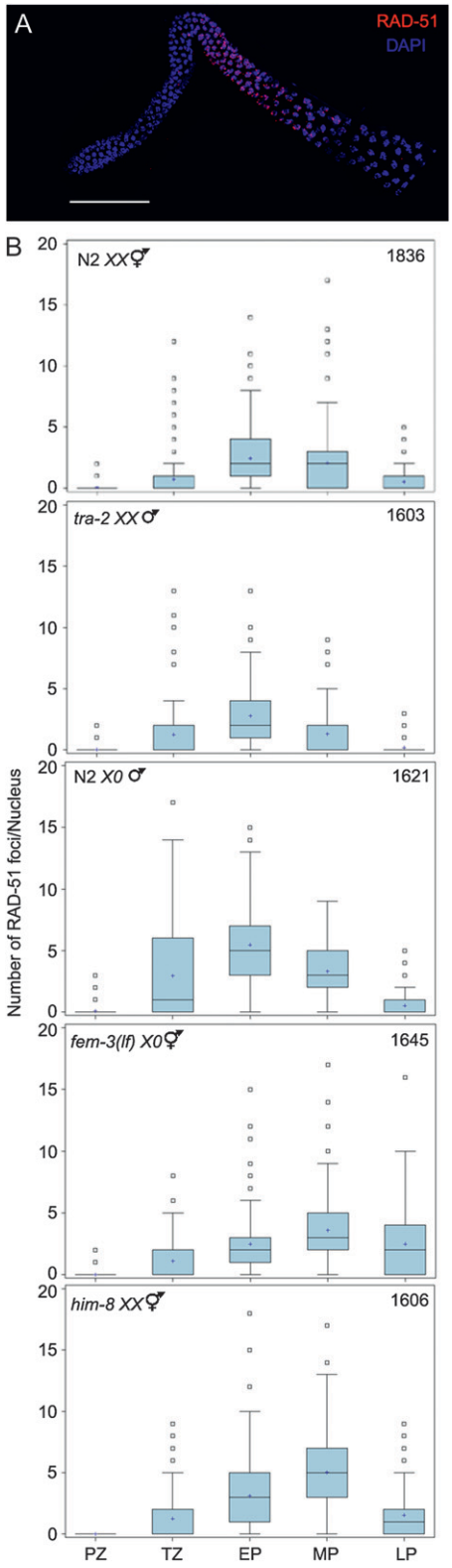

Figure 4.—Assembly and removal of RAD-51 foci during meiotic prophase progression. (A) Image of adult N2 *X0* gonad stained with DAPI (blue) and α-RAD-51 (red). Scale bar, 50 μm. (B) Quantification of RAD-51 focus formation in N2 *XX*, *tra-2(e1095) XX*, N2 *X0*, *fem-3(e1996) X0*, and *him-8(me4) XX*. Gonads were divided into prophase substages and nuclei assigned to each region on the basis of morphology and location. Graphs display box-whisker plots of focus numbers. *X*-axis indicates meiotic prophase stages: Proliferative zone (PZ), transition zone (TZ), early pachytene (EP), midpachytene (MP), and late pachytene (LP); *y*-axis indicates number of RAD-51 foci/nucleus. Center horizontal line of each box indicates the median measurements; lines extending above and below boxes indicate standard deviation and outliers indicate the entire range of measurements. Numbers of nuclei observed for each strain are indicated in upper right.

activation of checkpoints as it does in *him-8 XX* hermaphrodites (Table 1; Bhalla and Dernburg 2005).

HORMA domain proteins are loaded onto the single X chromosome: What is different about the single X chromosome that enables delayed repair of breaks using a sister chromatid as a template without eliciting a checkpoint response? In *Sacccharomyces cerevisiae*, Hop1, the meiosis-specific HORMA (Aravind and Koonin 1998) domain protein of the chromosomal axes (Hollingsworth *et al.* 1990), is essential for interhomolog bias during meiotic recombination (Niu *et al.* 2005). HIM-3, an ortholog of Hop1, associates with the chromosome core of both synapsed and asynapsed chromosomes in hermaphrodites (Zetka *et al.* 1999). In *him-3* mutants, recombination is initiated and breaks are repaired efficiently, despite the failure in synapsis, suggesting that HIM-3 also functions in interhomolog bias during meiotic recombination (Couteau *et al.* 2004). Interestingly, in *him-3* null mutant hermaphrodites there is no increase in apoptosis, suggesting that checkpoints are not activated even though there is chromosomal asynapsis and lack of a homologous chromosome for repair of DSBs (Couteau *et al.* 2004). During male meiosis, immunofluorescence studies revealed that the single X chromosome lacks HIM-3 staining at metaphase I (Zetka *et al.* 1999), suggesting that HIM-3's absence may explain the failure in checkpoint signaling. As metaphase I chromosomes have already completed recombination, we examined HIM-3 loading onto the X chromosome during meiotic prophase when recombination events are initiated and repaired. We observed HIM-3 on the single X chromosome in pachytene nuclei in the male germ line as well as in *fem-3(lf)* germ lines (Figure 5A, top three panels) (see also Shakes *et al.* 2009). Furthermore, in the *fem-3(lf) X0* mutant HIM-3 was maintained on the single X in diakinesis as in N2 *XX* hermaphrodites (bottom two panels).

In addition to HIM-3, *C. elegans* has three paralogous HORMA domain proteins that are structural components of the meiotic chromosome axes and have also been implicated in checkpoints: HTP-1, HTP-2 (Couteau and Zetka 2005; Martinez-Perez and Villeneuve 2005; Martinez-Perez *et al.* 2008), and HTP-3 (Goodyer *et al.* 2008). We monitored the assembly and disassembly of these proteins in hermaphrodite *XX*, male *X0*, and *fem-3(lf) X0* mutant germ lines and found that all of these proteins were loaded onto

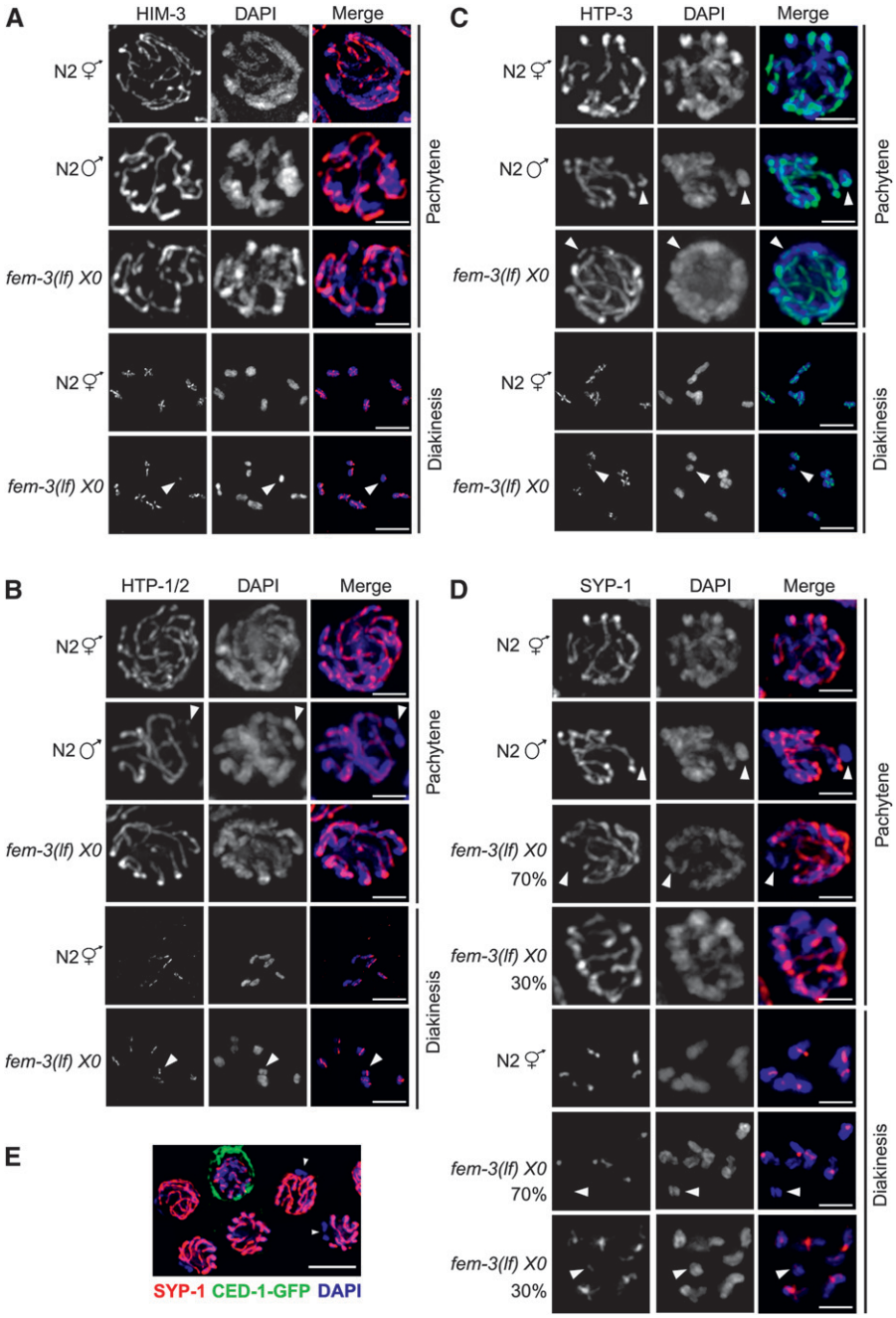

FIGURE 5.—Loading of SC axial and central elements onto the X chromosome(s). Immunolocalization of (A) HIM-3 (red), (B) HTP-1/2 (red), (C) HTP-3 (green), and (D) SYP-1 (red) counterstained with DAPI (blue) in nuclei from N2 *XX*, N2 *X0*, and *fem-3(e1996) X0* germ lines. Arrowheads point to X chromosome determined by lack of localization of SYP-1 or by size of DAPI staining body. Scale bar, 2 μm. (E) SYP-1 (red) and CED-1-GFP (green) localization in a *fem-3(e1996) X0* germ line. Arrowheads indicate chromosome lacking SYP-1. Scale bar, 5 μm.

both the paired Xs and the single X (Figure 5, B and C). Hence it is not the absence of HORMA domain axial components on the single X that prevents a checkpoint response.

Some *fem-3(lf)* X chromosomes achieve self-synapsis: We also monitored the loading of the SC central component, SYP-1, on the single X chromosome in pachytene (Figure 5D, top four panels) and diakinesis nuclei (Figure 5D, bottom three panels). SYP-1 was not loaded on the single X of N2 males; however, ~30% of *fem-3(lf)* X chromosomes had SYP-1 staining, suggesting that these chromosomes had achieved nonhomologous self-synapsis (Figure 5D; arrowheads denote X chromosome). This is analogous to what has been observed in the X0 mouse, where 30% of the X chromosomes engage in nonhomologous self-synapsis (SPEED 1986; TURNER *et al.* 2005).

The observation that some X chromosomes engage in self-synapsis suggested that these nuclei may escape detection by the checkpoint machinery and that this may account for the failure in checkpoint signaling in the *fem-3(lf) X0* mutant. To investigate this possibility, we simultaneously monitored apoptosis (using GFP antibodies) and SYP-1 by immunofluorescence in worms expressing CED-1-GFP (Figure 5E). We found that germ cell nuclei with SYP-1 and without SYP-1 on the X

chromosome were equally likely to undergo apoptosis, indicating that self-synapsis of the X does not prevent checkpoint signaling.

Transcriptional silencing of the single X chromosome late in prophase correlates with lack of checkpoint signaling: Asynapsed chromosomes, including the male X, accumulate the heterochromatin mark H3dimethylK9 to a greater extent than paired X chromosomes (Kelly *et al.* 2002; Bean *et al.* 2004). Further, the X chromosome pair becomes transcriptionally active for a set of oocyte-enriched genes late in pachytene while the single X remains silent in males (Reinke *et al.* 2000; Kelly *et al.* 2002). To investigate the relationship between chromatin/transcriptional state and checkpoint signaling, we monitored repressive and activating chromatin marks and X-linked gene transcription in N2 *XX* hermaphrodites, N2 *X0* males, *fem-3(lf) X0* females, and *him-8 XX* hermaphrodites. As previously reported, H3dimethylK9 is found predominantly on the paired X chromosomes in N2 hermaphrodite germ lines and accumulates on the single X in male and the asynapsed Xs in *him-8* hermaphrodite germ lines (Kelly *et al.* 2002; Bean *et al.* 2004). A single intense focus is also observed in the *fem-3(lf) X0* germ line, which presumably represents the unpaired X (Figure 6A). In N2 and *him-8* hermaphrodites, this mark is redistributed throughout the genome in the transition from pachytene to diplotene (Kelly *et al.* 2002; Bean *et al.* 2004). In N2 male germ lines, H3dimethylK9 persisted on the single X chromosome until the transition to spermatocytes (Figure 6A). In *fem-3(lf) X0* germ lines, the H3dimethylK9 foci remained intense until diakinesis, although there was some redistribution of the mark in diplotene (Figure 6A).

The release of H3dimethylK9 in hermaphrodites, but not in males, is accompanied by an accumulation of activating marks and the onset of transcription of a set of X-linked oocyte-enriched genes (Reinke *et al.* 2000; Kelly *et al.* 2002). It was noted that *him-8(e1489)* also loads activating marks on the asynapsed Xs late in prophase (Bean *et al.* 2004). Analysis of H3dimethylK4 showed that indeed this activating mark accumulated on the X chromosomes in both N2 and *him-8(me4)* hermaphrodites late in pachytene and was maintained through diakinesis (Figure 6B). In N2 *X0* and *fem-3(lf) X0* worms H3dimethylK4 was not found on the X in late pachytene but began to weakly stain the X at the transition to spermatocytes (N2 males) and at the transition to diplotene [*fem-3(lf) X0*] (Figure 6B). H3dimethylK4 labels all six DAPI-staining bodies of *fem-3(lf) X0* at diakinesis (Figure 6B).

To determine whether the late acquisition of activating marks correlated with lack of transcription, we performed *in situ* hybridization with two X-linked oocyte-enriched genes, which are activated in late pachytene in hermaphrodites (Kelly *et al.* 2002). As expected, N2 *XX* and *him-8(me4) XX* hermaphrodites exhibited expression of these genes in late pachytene extending to diakinesis (Figure 6C and data not shown). Expression was also observed in *him-8(e1489) XX* hermaphrodites (data not shown). In contrast, in the germ lines of both N2 *X0* males and *fem-3(lf) X0* females transcription of these genes was not activated (Figure 6C and data not shown). These results indicate that the single X in *fem-3(lf)* has chromatin/transcriptional properties similar to the single X in N2 males.

To further examine the relationship between chromatin state and checkpoint signaling, we monitored repressive H3dimethylK9 and activating H3dimethylK4 in *zim-2(tm574) XX* and *fem-3(lf); zim-2(RNAi) X0* worms, in which the recombination checkpoint is activated because of chromosome V asynapsis (Table 1). In *zim-2 XX* hermaphrodite germ lines, H3dimethylK9 was modestly enriched on two chromosomes, which presumably represent the unpaired Vs, in pachytene, and was redistributed throughout the nucleus in late pachytene-diplotene (Figure 6D). In *fem-3(lf); zim-2(RNAi) X0* germ lines, H3dimethylK9 was enriched on the X (marked with HIM-8) and also found on two chromosomes, presumably the unpaired Vs; H3dimethylK9 was retained only on the X into late pachytene-diplotene (Figure 6D). In contrast, H3dimethylK4 was observed on all chromosomes by late pachytene-diplotene in *zim-2 XX* mutants, but its acquisition was delayed on the single X in *fem-3(lf); zim-2(RNAi)* worms (Figure 6E). Taken together, these results suggest that it is the unique chromatin/transcriptional state of the X that enables heterogametic sex chromosomes to be hidden from the checkpoint machinery.

DISCUSSION

In this study, we show that both meiotic prophase kinetics and apoptosis are sexually dimorphic in *C. elegans*: germ lines undergoing oogenesis have slow prophase kinetics and both physiological and checkpoint-activated apoptosis. Contrastingly, germ lines undergoing spermatogenesis have fast prophase kinetics and lack germ-line apoptosis. Additionally, we found that meiotic DSBs are induced on the single X chromosome of wild-type males and the lack of a homologous chromosome to repair these breaks is sensed by the germ line but fails to induce apoptosis even in a background competent for checkpoint signaling. We also provide evidence that the chromatin/transcriptional state of a single X chromosome is distinct from unpaired X chromosomes or autosomes and suggest that this helps mask the X from the checkpoint machinery thereby preventing constitutive checkpoint activation.

Sex-dependent coordination of meiotic prophase kinetics and apoptosis: Slow meiotic prophase kinetics and apoptosis were observed in germ lines of worms

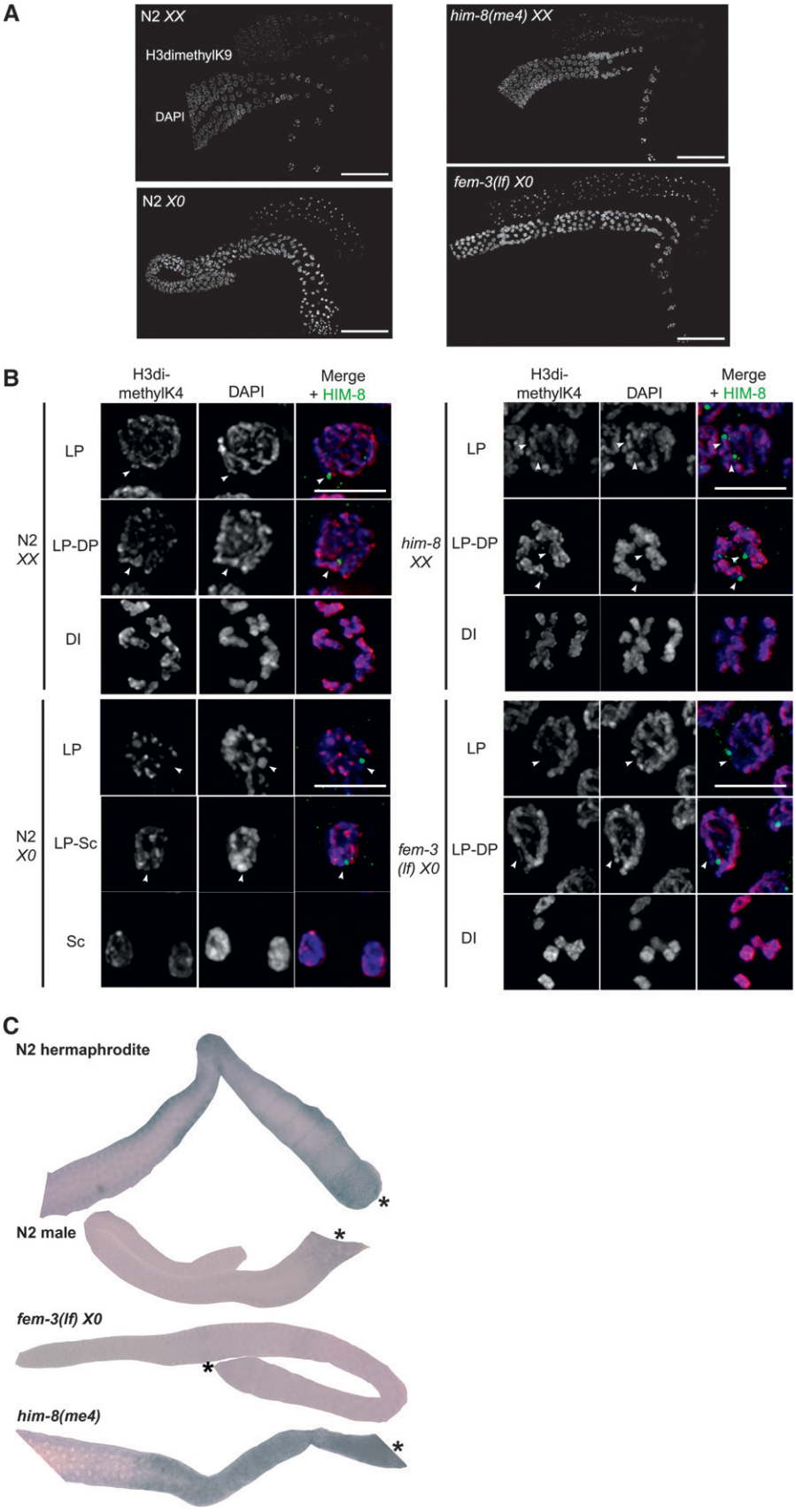

FIGURE 6.—Chromatin/transcriptional state of X chromosome(s). Immunolocalization of (A) H3dimethylK9; scale bar, 50 μm and (B) H3methylK4 (red) counterstained with DAPI (blue); scale bar, 5 μm in N2 *XX*, N2 *X0*, *fem-3(e1996) X0*, and *him-8(me4) XX* germ lines. Images were captured with same exposure time. Arrowheads indicate X chromosome(s) as determined by HIM-8 staining (green); HIM-8 is not present on diakinesis or spermatocyte nuclei. (C) In situ hybridization of oocyte-enriched X-linked F52D2.2 in N2 *XX*, N2 *X0*, *fem-3(e1996) X0*, and *him-8(me4) XX* germ lines. *fem-3(e1996) X0* worms were mated with N2 males. Asterisk denotes proximal gonad. (D) Immunolocalization of H3dimethylK9 (green) counterstained with DAPI (blue); scale bar, 5 μm in *zim-2(tm574) XX* and *fem-3(e1996); zim-2(RNAi) X0* germ lines. Arrowheads indicate X chromosome(s) (HIM-8; red); arrows indicate chromosomes with H3dimethlyK9 that presumably represent chromosome V. (E) H3methylK4 (red) counterstained with DAPI (blue); scale bar, 5 μm in *zim-2(tm574) XX* and *fem-3(e1996); zim-2(RNAi) X0* germ lines. Arrowheads indicate X chromosome(s) (HIM-8; green). Late pachytene (LP), diplotene (DP), diakinesis (DI), and spermatocyte (Sc).

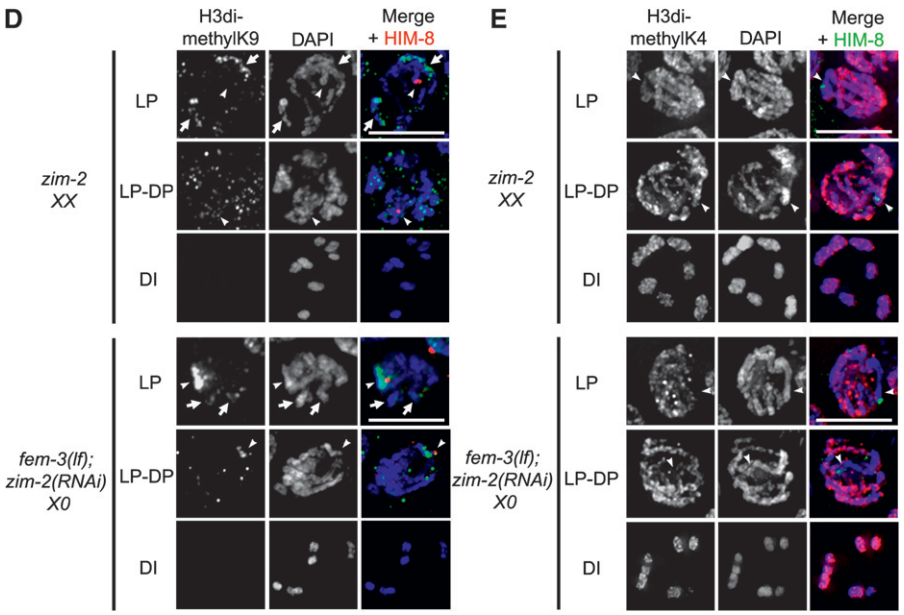

Figure 6.—*Continued.*

undergoing oogenesis regardless of the soma or X chromosome constitution, suggesting that these processes are important for formation of functional oocytes, but not sperm, and are coordinately regulated. As in many organisms, *C. elegans* oocytes are significantly larger than sperm as oocytes must incorporate yolk lipoproteins, maternal mRNAs, and other cellular components required for early embryogenesis (Hall *et al.* 1999). In contrast, during spermatogenesis the developing spermatids bud from a central residual body where most of the cellular components are left behind (L'hernault 2006). Thus, it is not surprising that the most striking difference in meiotic prophase timing in the sexes is observed at pachytene (Jaramillo-Lambert *et al.* 2007). Apoptosis also occurs at pachytene and has been proposed to serve a nurse cell function by contributing to the pool of cellular components ultimately packaged into oocytes (Gumienny *et al.* 1999; Wolke *et al.* 2007; Andux and Ellis 2008). Furthermore, physiological apoptosis plays a maternal age-dependent role in oocyte quality, while the quality of sperm is not affected by paternal age (Andux and Ellis 2008).

MAP kinase pathways play integral roles in controlling and coordinating several aspects of female and male germ-line biology including meiotic prophase progression, apoptosis, and sexual fate (Lee *et al.* 2007). In *C. elegans* hermaphrodites, sustained activation of MAP kinase, MPK-1, is needed for germ cells to transition through pachytene (Greenstein 2005; Lee *et al.* 2007). MPK-1 was originally reported to also function in pachytene progression in the male germ line as loss-of-function alleles of *mpk-1* resulted in a male pachytene arrest phenotype (Church *et al.* 1995). However, genetic and cellular analyses revealed that MPK-1 functions to promote male germ cell fate and the observed pachytene arrest in *mpk-1* males was due to feminization of the germ line (Lee *et al.* 2007). Thus, it is unlikely that MPK-1 is required in the male germ line for cells to transit pachytene as MPK-1 is not present in this region of the germ line. The presence of MPK-1 in the pachytene region of hermaphrodite but not male germ lines may also explain the lack of apoptosis in the male germ line. If so, then one prediction is that expression of MPK-1 in the pachytene region of the male germ line would both slow meiotic prophase progression and promote germ-line apoptosis.

Sex-specific differences in meiotic prophase timing and germ-line apoptosis may also influence the phenotypic outcome of meiotic mutants. Mutations of essential meiotic components result in sexually dimorphic phenotypes in mammals. For example, mutations of SC components and proteins involved in DSB repair result in male sterility with meiosis unable to proceed beyond zygonema and a subsequent culling of germ cells by apoptosis, while female mutants show reduced fertility with oocytes that progress beyond pachynema (Morelli and Cohen 2005). *C. elegans* meiotic mutants also display sexually dimorphic phenotypes. Disruption of the sister chromatid cohesin REC-8 results in precocious separation of sister chromatids (Pasierbek *et al.* 2001). Surprisingly, progeny from *rec-8* hermaphrodites mated to wild-type males have a high hatch rate (89%) while only 16% of embryos hatch when the sperm come from *rec-8* males (Severson *et al.* 2009). Mutations that disrupt chromosome synapsis or recombinational repair in either hermaphrodites or males result in extensive embryonic lethality, but only the adult hermaphrodite germ line responds by inducing apoptosis (MacQueen *et al.* 2002; Alpi *et al.* 2003; Colaiácovo *et al.* 2003; Smolikov *et al.* 2007, 2009). Perhaps, a lengthier prophase in hermaphrodites gives the germ

line time to launch a checkpoint response, which allows for DNA damage repair, or to remove defective germ cells. Interestingly, more progeny survive when sperm are *spo-11* deficient (20% hatching) than when oocytes come from *spo-11* mothers (11%) (Severson *et al.* 2009). SPO-11 is a conserved topisomerase responsible for initiating meiotic DSBs; in *spo-11* mutants there are no breaks and consequently checkpoints are not activated (Dernburg *et al.* 1998; MacQueen *et al.* 2002; Bhalla and Dernburg 2005). That *spo-11* produce sperm with the correct ploidy more often than oocytes suggest that achiasmatic chromosomes are segregated more effectively in males than in hermaphrodites and may explain why hermaphrodites, but not males, have active checkpoint pathways.

Asynapsed chromosomes, sex, and meiotic checkpoints: Errors in chromosomal synapsis often lead to removal of germ cells by apoptosis (Bhalla and Dernburg 2005; Morelli and Cohen 2005; Burgoyne *et al.* 2009). The X chromosome of *C. elegans* males lacks a pairing partner, a situation that triggers checkpoint-activated apoptosis in hermaphrodites. However, N2 *X0* males do not have physiological apoptosis (Gumienny *et al.* 1999) nor do they respond to chromosomal asynapsis by inducing apoptosis (Figure 2B; Table 1), thereby preventing elimination of all germ cells. On the other hand, *fem-3(lf) X0* and *fog-1(lf) X0* germ lines have elevated levels of apoptosis in response to autosomal asynapsis but have low levels of apoptosis under physiological conditions (Figure 2A and Table 1), suggesting that they do not recognize the X as unpaired. Consistent with this, depletion of either *pch-2*, required for the synapsis checkpoint (Bhalla and Dernburg 2005), or *chk-1*, which functions in the recombination and DNA damage checkpoints (Rhind and Russell 2000), had no affect on apoptotic levels, suggesting that neither the synapsis nor the recombination checkpoint pathways is activated in these worms. That the levels of basal apoptosis were lower than wild type is most likely a consequence of a reduction in meiotic maturation as *fem-3(e1996) X0* females do not produce sperm (Hodgkin 1986). Major sperm protein (MSP) promotes meiotic maturation and the absence of sperm causes oocytes to arrest at diakinesis (McCarter *et al.* 1999). Although we mated *fem-3(lf) X0* females with N2 males prior to quantification of apoptosis to provide a source of MSP, these females tended to have more oocytes than N2 hermaphrodites, suggesting that meiotic maturation had been delayed.

In the *C. elegans* germ line, unrepaired recombination intermediates are detected by the 9-1-1 (Rad9-Rad1-Hus1) complex and the P-I-3-kinase-related protein kinases, ATM and ATR (Hofmann *et al.* 2002; Garcia-Muse and Boulton 2005). CHK-1 functions downstream of ATR/ATM to transduce the checkpoint signal to the apoptotic machinery via phosphorylation of the p53 homolog, CEP-1 (Rhind and Russell 2000). Checkpoint-activated apoptosis due to activation of the synapsis checkpoint is mediated through the AAA-ATPase, PCH-2, independently of CEP-1 (Bhalla and Dernburg 2005; Phillips and Dernburg 2006); however, how PCH-2 relays the signal has not been elucidated. Consistent with a previous study, our analysis of apoptosis in N2 *XX* hermaphrodites and *fem-3(lf) X0* germ lines revealed that depletion of PCH-2 when chromosomal asynapsis is induced results in intermediate levels of apoptosis (Table 1) (Bhalla and Dernburg 2005), as the recombination checkpoint is also activated when chromosome synapsis is impaired (Bhalla and Dernburg 2005). Surprisingly, knockdown of CHK-1 in the presence of chromosomal asynapsis reduced the number of apoptotic nuclei to physiological levels (Table 1), suggesting that the PCH-2 synapsis checkpoint signal is transmitted to the apoptotic machinery through CHK-1. The interconnection between the recombination and synapsis checkpoint signaling pathways awaits further characterization.

Heterogametic sex chromosomes and checkpoint signaling: We have shown that the single X chromosome of males and *fem-3(lf)* animals incur DSBs and that the absence of a homologous chromosome is detected by the germ line as evidenced by increased levels of RAD-51 foci on all chromosomes and a delay in the disappearance in these foci (Figures 3 and 4). Male genetic recombination frequencies have been reported to be reduced (Zetka and Rose 1990; Meneely *et al.* 2002) or the same as hermaphrodites (Lim *et al.* 2008), yet we observed an increase in the levels of RAD-51 foci in the male compared to hermaphrodite germ line. This apparent discrepancy is most likely because we are only looking at a single point in time and the levels of RAD-51 foci reflect both the number of breaks and repair kinetics. Furthermore, some of the breaks may be repaired as noncrossovers, which would not influence the genetic map distance. Nevertheless, it appears that germ lines with a single X chromosome sense the absence of a homologous chromosome but do not activate checkpoints. Early in meiosis, a bias is established to promote the use of the homolog to repair DSBs. The interhomolog bias is mediated through axial components of the SC, which have also been implicated in checkpoint function (Zetka *et al.* 1999; Couteau and Zetka 2005; Martinez-Perez and Villeneuve 2005; Niu *et al.* 2005;Goodyer *et al.* 2008; Martinez-Perez *et al.* 2008). One possibility is that the single X chromosome evades checkpoint detection through an early release in the bias to allow repair of DSBs via the sister chromatid. Our examination of HIM-3, HTP-1/2, and HTP-3 localization revealed that these proteins are retained on the X chromosome core throughout prophase consistent with the delay in removal of RAD-51 foci, and thus early release of these axial components is unlikely to explain the lack of checkpoint signaling. However, it is possible that other proteins associated

with the axis or post-translational modifications of these axial components are different on the single X compared to either asynapsed Xs or autosomes and may contribute to the ability of the single X to evade detection by the checkpoint machinery.

Analysis of chromatin marks and X-linked gene expression suggests that the chromatin/transcriptional status of X may distinguish the lone X from asynapsed chromosomes to prevent inappropriate checkpoint activation. We found that while the lone X in *fem-3(lf)* mutants, the asynapsed Xs in *him-8*, and the asynapsed Vs in *zim-2* accumulate H3dimethylK9, a repressive mark associated with heterochromatin (Kelly *et al.* 2002), only the asynapsed chromosome pairs accumulate activating marks late in pachytene, induce gene expression, and activate checkpoints. Bean *et al.* (2004) suggested that the acquisition of activating marks in *him-8* was a consequence of low levels of pairing observed in the *him-8(e1489)* mutant. However, both *him-8(e1489)* and *him-8(me4)* have as severe pairing defects as the deletion allele (Phillips *et al.* 2005). We suggest that late acquisition of activating marks and lack of gene transcription of the single X chromosome prevents detection of the unpaired X by the checkpoint machinery. Alternatively, upstream pathways that respond to X chromosome number, such as the dosage compensation machinery (Meyer 2005) or the *mes* (maternal-effect sterile) genes (Garvin *et al.* 1998), may function to block checkpoint signaling when the X is unpaired in addition to influencing the transcriptional status of the X.

In mammalian males, there is also accumulation of H3dimethylK9 and transcriptional silencing of the X and Y chromosomes (Namekawa *et al.* 2006). It was proposed that MSCI is related to general silencing of unpaired DNA or MSUC. Consistent with this, in both *C. elegans* and mammals unpaired autosomes as well as the sex chromosomes attract H3dimethylK9 (Bean *et al.* 2004; Schimenti 2005; Figure 6). However, MSCI of the single X in *C. elegans* males appears to be a more stable transcriptionally repressed state than unpaired Xs or autosomes in hermaphrodites. Transcriptional repression of the single X suggests the possibility that there is an X-linked gene required in *trans* for checkpoint signaling that is not expressed in males. However, we do not favor this hypothesis as checkpoint activation occurs in *fem-3(lf) X0* worms in the presence of asynapsed autosomes even though there is transcriptional repression of the X. Our results instead suggest that transcriptional repression of the X functions in *cis* to prevent detection of the asynapsed X by the checkpoint machinery. Further analyses of chromatin modifications, transcriptional profiles and upstream pathways will need to be performed to determine the relationship between the transcriptional status of the single X chromosome and checkpoint signaling.

It was previously proposed that the single X chromosome of *C. elegans* males is analogous to the sex body in mammals (Kelly *et al.* 2002). In mammalian spermatogenesis the sex body is transcriptionally silenced and is separated from the autosomes in its own nuclear domain (Handel 2004; Turner *et al.* 2005). In addition to the accumulation of H3dimethylK9, the sex body chromatin domain also accumulates BRCA1, ATR, and the phosphorylated form of H2AX, γH2AX; proteins essential for MSCI but are also involved in checkpoints (Turner *et al.* 2004, 2005). BRCA1 is not required for X silencing in *C. elegans* males but its localization pattern has not been determined (Kelly and Aramayo 2007). On the other hand, while ATR is required for DNA damage checkpoint signaling in *C. elegans* (Garcia-Muse and Boulton 2005) it does not accumulate on the single X chromosome of males (A. Jaramillo-Lambert and J. Engebrecht, unpublished results) and H2AX is not found in *C. elegans* (Boulton 2006; Kelly and Aramayo 2007). It appears that in mammalian male germ cells, the sex body is recognized as unpaired; ATR and γH2AX are recruited to the sex body, but the checkpoint machinery has been assimilated to function in transcriptional silencing and does not promote checkpoint activation in this context. The single X chromosome of *C. elegans* males is transcriptionally silenced, but does not recruit checkpoint proteins and nonetheless evades checkpoint activation. While checkpoint proteins are not required for transcriptional silencing in *C. elegans*, the same transcriptional silencing and checkpoint evasion outcome is achieved similarly to what occurs in the male mammalian germ line.

We thank A. Dernburg, A. Villeneuve, and M. Zetka for generously providing antibodies. We also thank T. Schedl and the Caenorhabditis Genetic Center for strains and helpful discussion and S. Burgess, D. Starr, and J. Vitt for comments on the manuscript. This work was supported by National Institutes of Health (NIH) GM086505 and the Agricultural Experimental Station CA-D*MCB-7237-H (to J.E.). A.J.L. was supported by NIH T32GM070377 and a University of California, Davis Office of Graduate Studies dissertation-year fellowship.

LITERATURE CITED

Alpi, A., P. Pasierbek, A. Gartner and J. Loidl, 2003 Genetic and cytological characterization of the recombination protein RAD-51 in *Caenorhabditis elegans*. Chromosoma **112:** 6–16.

Andux, S., and R. E. Ellis, 2008 Apoptosis maintains oocyte quality in aging *Caenorhabditis elegans* females. PLoS Genet. **4:** e1000295.

Aravind, L., and E. V. Koonin, 1998 The HORMA domain: a common structural denominator in mitotic checkpoints, chromosome synapsis and DNA repair. Trends Biochem. Sci. **23:** 284–286.

Ashley, T., A. W. Plug, J. Xu, A. J. Solari, G. Reddy *et al.*, 1995 Dynamic changes in Rad51 distribution on chromatin during meiosis in male and female vertebrates. Chromosoma **104:** 19–28.

Barton, M. K., and J. Kimble, 1990 *fog-1*, a regulatory gene required for specification of spermatogenesis in the germ line of *Caenorhabditis elegans*. Genetics **125:** 29–39.

Barton, M. K., T. B. Schedl and J. Kimble, 1987 Gain-of-function mutations of *fem-3*, a sex-determination gene in *Caenorhabditis elegans*. Genetics **115:** 107–119.

Bean, C. J., C. E. Schaner and W. G. Kelly, 2004 Meiotic pairing and imprinted X chromatin assembly in *Caenorhabditis elegans*. Nat. Genet. **36:** 100–105.

Bhalla, N., and A. F. Dernburg, 2005 A conserved checkpoint monitors meiotic chromosome synapsis in *Caenorhabditis elegans*. Science **310:** 1683–1686.

Blank, R. D., G. R. Campbell, A. Calabro and P. D'Eustachio, 1988 A linkage map of mouse chromosome 12: localization of Igh and effects of sex and interference on recombination. Genetics **120:** 1073–1083.

Boulton, S. J., 2006 BRCA1-mediated ubiquitylation. Cell Cycle **5:** 1481–1486.

Boulton, S. J., J. S. Martin, J. Polanowska, D. E. Hill, A. Gartner *et al.*, 2004 BRCA1/BARD1 orthologs required for DNA repair in *Caenorhabditis elegans*. Curr. Biol. **14:** 33–39.

Brenner, S., 1974 The genetics of *Caenorhabditis elegans*. Genetics **77:** 71–94.

Burgoyne, P. S., S. K. Mahadevaiah and J. M. Turner, 2009 The consequences of asynapsis for mammalian meiosis. Nat. Rev. Genet. **10:** 207–216.

Carlton, P. M., A. P. Farruggio and A. F. Dernburg, 2006 A link between meiotic prophase progression and crossover control. PLoS Genet. **2:** e12.

Church, D. L., K. L. Guan and E. J. Lambie, 1995 Three genes of the MAP kinase cascade, *mek-2, mpk-1/sur-1* and *let-60* ras, are required for meiotic cell cycle progression in *Caenorhabditis elegans*. Development **121:** 2525–2535.

Colaiácovo, M. P., A. J. MacQueen, E. Martinez-Perez, K. McDonald, A. Adamo *et al.*, 2003 Synaptonemal complex assembly in *C. elegans* is dispensable for loading strand-exchange proteins but critical for proper completion of recombination. Dev. Cell **5:** 463–474.

Couteau, F., K. Nabeshima, A. Villeneuve and M. Zetka, 2004 A component of *C. elegans* meiotic chromosome axes at the interface of homolog alignment, synapsis, nuclear reorganization, and recombination. Curr. Biol. **14:** 585–592.

Couteau, F., and M. Zetka, 2005 HTP-1 coordinates synaptonemal complex assembly with homolog alignment during meiosis in *C. elegans*. Genes Dev. **19:** 2744–2756.

Dernburg, A. F., K. McDonald, G. Moulder, R. Barstead, M. Dresser *et al.*, 1998 Meiotic recombination in *C. elegans* initiates by a conserved mechanism and is dispensable for homologous chromosome synapsis. Cell **94:** 387–398.

Donis-Keller, H., P. Green, C. Helms, S. Cartinhour, B. Weiffenbach *et al.*, 1987 A genetic linkage map of the human genome. Cell **51:** 319–337.

Eppig, J. J., R. M. Schultz and G. S. Kopf, 1996 Maturation of mouse oocytes in serum-free medium. Hum. Reprod. **11:** 1139–1140.

Garcia-Muse, T., and S. J. Boulton, 2005 Distinct modes of ATR activation after replication stress and DNA double-strand breaks in *Caenorhabditis elegans*. EMBO J. **24:** 4345–4355.

Gartner, A., A. J. MacQueen and A. M. Villeneuve, 2004 Methods for analyzing checkpoint responses in *Caenorhabditis elegans*. Methods Mol. Biol. **280:** 257–274.

Gartner, A., S. Milstein, S. Ahmed, J. Hodgkin and M. O. Hengartner, 2000 A conserved checkpoint pathway mediates DNA damage-induced apoptosis and cell cycle arrest in *C. elegans*. Mol. Cell **5:** 435–443.

Garvin, C., R. Holdeman and S. Strome, 1998 The phenotype of *mes-2, mes-3, mes-4* and *mes-6*, maternal-effect genes required for survival of the germline in *Caenorhabditis elegans*, is sensitive to chromosome dosage. Genetics **148:** 167–185.

Goodyer, W., S. Kaitna, F. Couteau, J. D. Ward, S. J. Boulton *et al.*, 2008 HTP-3 links DSB formation with homolog pairing and crossing over during *C. elegans* meiosis. Dev. Cell **14:** 263–274.

Greenstein, D., 2005 Control of oocyte meiotic maturation and fertilization. WormBook, 1–12.

Gumienny, T. L., E. Lambie, E. Hartwieg, H. R. Horvitz and M. O. Hengartner, 1999 Genetic control of programmed cell death in the *Caenorhabditis elegans* hermaphrodite germline. Development **126:** 1011–1022.

Hall, D. H., V. P. Winfrey, G. Blaeuer, L. H. Hoffman, T. Furuta *et al.*, 1999 Ultrastructural features of the adult hermaphrodite gonad of *Caenorhabditis elegans*: relations between the germ line and soma. Dev. Biol. **212:** 101–123.

Handel, M. A., 2004 The XY body: a specialized meiotic chromatin domain. Exp. Cell Res. **296:** 57–63.

Handel, M. A., and J. J. Eppig, 1998 Sexual dimorphism in the regulation of mammalian meiosis. Curr. Top. Dev. Biol. **37:** 333–358.

Harrison, J. C., and J. E. Haber, 2006 Surviving the breakup: the DNA damage checkpoint. Annu. Rev. Genet. **40:** 209–235.

Hassold, T., and P. Hunt, 2001 To err (meiotically) is human: the genesis of human aneuploidy. Nat. Rev. Genet. **2:** 280–291.

Hochwagen, A., and A. Amon, 2006 Checking your breaks: surveillance mechanisms of meiotic recombination. Curr. Biol. **16:** R217–R228.

Hodgkin, J., 1986 Sex determination in the nematode *C. elegans*: analysis of *tra-3* suppressors and characterization of *fem* genes. Genetics **114:** 15–52.

Hodgkin, J. A., and S. Brenner, 1977 Mutations causing transformation of sexual phenotype in the nematode *Caenorhabditis elegans*. Genetics **86:** 275–287.

Hofmann, E. R., S. Milstein, S. J. Boulton, M. Ye, J. J. Hofmann *et al.*, 2002 *Caenorhabditis elegans* HUS-1 is a DNA damage checkpoint protein required for genome stability and EGL-1-mediated apoptosis. Curr. Biol. **12:** 1908–1918.

Hollingsworth, N. M., L. Goetsch and B. Byers, 1990 The *HOP1* gene encodes a meiosis-specific component of yeast chromosomes. Cell **61:** 73–84.

Hubbard, E. J., and D. Greenstein, 2005 Introduction to the germ line. WormBook, 1–4.

Hunt, P. A., and T. J. Hassold, 2002 Sex matters in meiosis. Science **296:** 2181–2183.

Jaramillo-Lambert, A., M. Ellefson, A. M. Villeneuve and J. Engebrecht, 2007 Differential timing of S phases, X chromosome replication, and meiotic prophase in the *C. elegans* germ line. Dev. Biol. **308:** 206–221.

Kamath, R. S., A. G. Fraser, Y. Dong, G. Poulin, R. Durbin *et al.*, 2003 Systematic functional analysis of the *Caenorhabditis elegans* genome using RNAi. Nature **421:** 231–237.

Kelly, W. G., and R. Aramayo, 2007 Meiotic silencing and the epigenetics of sex. Chromosome Res. **15:** 633–651.

Kelly, W. G., C. E. Schaner, A. F. Dernburg, M. H. Lee, S. K. Kim *et al.*, 2002 X-chromosome silencing in the germline of *C. elegans*. Development **129:** 479–492.

Kleckner, N., 1996 Meiosis: how could it work? Proc. Natl. Acad. Sci. USA **93:** 8167–8174.

Koehler, K. E., C. L. Boulton, H. E. Collins, R. L. French, K. C. Herman *et al.*, 1996 Spontaneous X chromosome MI and MII nondisjunction events in *Drosophila melanogaster* oocytes have different recombinational histories. Nat. Genet. **14:** 406–414.

L'Hernault, S. W., 2006 Spermatogenesis. WormBook, 1–14.

Lamb, N. E., S. B. Freeman, A. Savage-Austin, D. Pettay, L. Taft *et al.*, 1996 Susceptible chiasmate configurations of chromosome 21 predispose to non-disjunction in both maternal meiosis I and meiosis II. Nat. Genet. **14:** 400–405.

Lee, B., and A. Amon, 2001 Meiosis: how to create a specialized cell cycle. Curr. Opin. Cell Biol. **13:** 770–777.

Lee, M. H., and T. Schedl, 2006 RNA in situ hybridization of dissected gonads. WormBook, 1–7.

Lee, M. H., M. Ohmachi, S. Arur, S. Nayak, R. Francis *et al.*, 2007 Multiple functions and dynamic activation of MPK-1 extracellular signal-regulated kinase signaling in *Caenorhabditis elegans* germline development. Genetics **177:** 2039–2062.

Levine, A. J., 1997 p53, the cellular gatekeeper for growth and division. Cell **88:** 323–331.

Lim, J. G., R. R. Stine and J. L. Yanowitz, 2008 Domain-specific regulation of recombination in *Caenorhabditis elegans* in response to temperature, age and sex. Genetics **180:** 715–726.

MacQueen, A. J., M. P. Colaiacovo, K. McDonald and A. M. Villeneuve, 2002 Synapsis-dependent and -independent mechanisms stabilize homolog pairing during meiotic prophase in *C. elegans*. Genes Dev. **16:** 2428–2442.

MacQueen, A. J., C. M. Phillips, N. Bhalla, P. Weiser, A. M. Villeneuve *et al.*, 2005 Chromosome sites play dual roles to

establish homologous synapsis during meiosis in *C. elegans*. Cell **123:** 1037–1050.

Madl, J. E., and R. K. Herman, 1979 Polyploids and sex determination in *Caenorhabditis elegans*. Genetics **93:** 393–402.

Mahadevaiah, S. K., D. Bourc'his, D. G. de Rooij, T. H. Bestor, J. M. Turner *et al.*, 2008 Extensive meiotic asynapsis in mice antagonises meiotic silencing of unsynapsed chromatin and consequently disrupts meiotic sex chromosome inactivation. J. Cell Biol. **182:** 263–276.

Manandhar, G., H. Schatten and P. Sutovsky, 2005 Centrosome reduction during gametogenesis and its significance. Biol. Reprod. **72:** 2–13.

Martinez-Perez, E., M. Schvarzstein, C. Barroso, J. Lightfoot, A. F. Dernburg *et al.*, 2008 Crossovers trigger a remodeling of meiotic chromosome axis composition that is linked to two-step loss of sister chromatid cohesion. Genes Dev. **22:** 2886–2901.

Martinez-Perez, E., and A. M. Villeneuve, 2005 HTP-1-dependent constraints coordinate homolog pairing and synapsis and promote chiasma formation during *C. elegans* meiosis. Genes Dev. **19:** 2727–2743.

Masui, Y., and H. J. Clarke, 1979 Oocyte maturation. Int. Rev. Cytol. **57:** 185–282.

McCarter, J., B. Bartlett, T. Dang and T. Schedl, 1999 On the control of oocyte meiotic maturation and ovulation in *Caenorhabditis elegans*. Dev. Biol. **205:** 111–128.

Meneely, P. M., A. F. Farago and T. M. Kauffman, 2002 Crossover distribution and high interference for both the X chromosome and an autosome during oogenesis and spermatogenesis in *Caenorhabditis elegans*. Genetics **162:** 1169–1177.

Meyer, B. J., 2005 X–Chromosome dosage compensation. WormBook, 1–14.

Moens, P. B., D. J. Chen, Z. Shen, N. Kolas, M. Tarsounas *et al.*, 1997 Rad51 immunocytology in rat and mouse spermatocytes and oocytes. Chromosoma **106:** 207–215.

Morelli, M. A., and P. E. Cohen, 2005 Not all germ cells are created equal: aspects of sexual dimorphism in mammalian meiosis. Reproduction **130:** 761–781.

Morgan, T. H., 1912 Special Articles. Science **36:** 718–720.

Namekawa, S. H., P. J. Park, L. F. Zhang, J. E. Shima, J. R. McCarrey *et al.*, 2006 Postmeiotic sex chromatin in the male germline of mice. Curr. Biol. **16:** 660–667.

Niu, H., L. Wan, B. Baumgartner, D. Schaefer, J. Loidl *et al.*, 2005 Partner choice during meiosis is regulated by Hop1-promoted dimerization of Mek1. Mol. Biol. Cell. **16:** 5804–5818.

Page, J., A. Viera, M. T. Parra, R. de la Fuente, J. A. Suja *et al.*, 2006 Involvement of synaptonemal complex proteins in sex chromosome segregation during marsupial male meiosis. PLoS Genet. **2:** e136.

Pasierbek, P., M. Jantsch, M. Melcher, A. Schleiffer, D. Schweizer *et al.*, 2001 A *Caenorhabditis elegans* cohesion protein with functions in meiotic chromosome pairing and disjunction. Genes Dev. **15:** 1349–1360.

Perry, J., S. Palmer, A. Gabriel and A. Ashworth, 2001 A short pseudoautosomal region in laboratory mice. Genome Res. **11:** 1826–1832.

Phillips, C. M., and A. F. Dernburg, 2006 A family of zinc-finger proteins is required for chromosome-specific pairing and synapsis during meiosis in *C. elegans*. Dev. Cell **11:** 817–829.

Phillips, C. M., C. Wong, N. Bhalla, P. M. Carlton, P. Weiser *et al.*, 2005 HIM-8 binds to the X chromosome pairing center and mediates chromosome-specific meiotic synapsis. Cell **123:** 1051–1063.

Reinke, V., H. E. Smith, J. Nance, J. Wang, C. Van Doren *et al.*, 2000 A global profile of germline gene expression in *C. elegans*. Mol. Cell **6:** 605–616.

Rhind, N., and P. Russell, 2000 Chk1 and Cds1: linchpins of the DNA damage and replication checkpoint pathways. J. Cell Sci. **113**(Pt 22): 3889–3896.

Roeder, G. S., 1997 Meiotic chromosomes: it takes two to tango. Genes Dev. **11:** 2600–2621.

Ross, L. O., R. Maxfield and D. Dawson, 1996 Exchanges are not equally able to enhance meiotic chromosome segregation in yeast. Proc. Natl. Acad. Sci. USA **93:** 4979–4983.

Schimenti, J., 2005 Synapsis or silence. Nat. Genet. **37:** 11–13.

Schoenmakers, S., E. Wassenaar, J. W. Hoogerbrugge, J. S. Laven, J. A. Grootegoed *et al.*, 2009 Female meiotic sex chromosome inactivation in chicken. PLoS Genet. **5:** e1000466.

Severson, A. F., L. Ling, V. van Zuylen and B. J. Meyer, 2009 The axial element protein HTP-3 promotes cohesin loading and meiotic axis assembly in *C. elegans* to implement the meiotic program of chromosome segregation. Genes Dev. **23:** 1763–1778.

Shakes, D. C., J. C. Wu, P. L. Sadler, K. Laprade, L. L. Moore *et al.*, 2009 Spermatogenesis-specific features of the meiotic program in *Caenorhabditis elegans*. PLoS Genet. **5:** e1000611.

Singer, A., H. Perlman, Y. Yan, C. Walker, G. Corley-Smith *et al.*, 2002 Sex-specific recombination rates in zebrafish (*Danio rerio*). Genetics **160:** 649–657.

Smolikov, S., A. Eizinger, A. Hurlburt, E. Rogers, A. M. Villeneuve *et al.*, 2007 Synapsis-defective mutants reveal a correlation between chromosome conformation and mode of double-strand break repair during *Caenorhabditis elegans* meiosis. Genetics **176:** 2027–2033.

Smolikov, S., K. Schild-Prufert and M.P. Colaiacovo, 2009 A yeast two-hybrid screen for SYP-3 interactors identifies SYP-4, a component required for synaptonemal complex assembly and chiasma formation in *Caenorhabditis elegans* meiosis. PLoS Genet. **5:** e1000669.

Speed, R. M., 1986 Oocyte development in XO foetuses of man and mouse: the possible role of heterologous X-chromosome pairing in germ cell survival. Chromosoma **94:** 115–124.

Stergiou, L., K. Doukoumetzidis, A. Sendoel and M. O. Hengartner, 2007 The nucleotide excision repair pathway is required for UV-C-induced apoptosis in *Caenorhabditis elegans*. Cell Death Differ. **14:** 1129–1138.

Timmons, L., D. L. Court and A. Fire, 2001 Ingestion of bacterially expressed dsRNAs can produce specific and potent genetic interference in *Caenorhabditis elegans*. Gene **263:** 103–112.

Turner, J. M., O. Aprelikova, X. Xu, R. Wang, S. Kim *et al.*, 2004 BRCA1, histone H2AX phosphorylation, and male meiotic sex chromosome inactivation. Curr. Biol. **14:** 2135–2142.

Turner, J. M., S. K. Mahadevaiah, O. Fernandez-Capetillo, A. Nussenzweig, X. Xu *et al.*, 2005 Silencing of unsynapsed meiotic chromosomes in the mouse. Nat. Genet. **37:** 41–47.

Walworth, N. C., and R. Bernards, 1996 rad-dependent response of the chk1-encoded protein kinase at the DNA damage checkpoint. Science **271:** 353–356.

Wignall, S. M., and A. M. Villeneuve, 2009 Lateral microtubule bundles promote chromosome alignment during acentrosomal oocyte meiosis. Nat. Cell Biol. **11:** 839–844.

Wolke, U., E. A. Jezuit and J. R. Priess, 2007 Actin-dependent cytoplasmic streaming in *C. elegans* oogenesis. Development **134:** 2227–2236.

Wu, T. F., and D. S. Chu, 2008 Sperm chromatin: fertile grounds for proteomic discovery of clinical tools. Mol. Cell Proteomics **7:** 1876–1886.

Zetka, M. C., and A. M. Rose, 1990 Sex-related differences in crossing over in *Caenorhabditis elegans*. Genetics **126:** 355–363.

Zetka, M. C., I. Kawasaki, S. Strome and F. Muller, 1999 Synapsis and chiasma formation in *Caenorhabditis elegans* require HIM-3, a meiotic chromosome core component that functions in chromosome segregation. Genes Dev. **13:** 2258–2270.

Zhou, Z., E. Hartwieg and H. R. Horvitz, 2001 CED-1 is a transmembrane receptor that mediates cell corpse engulfment in *C. elegans*. Cell **104:** 43–56.

Zickler, D., and N. Kleckner, 1999 Meiotic chromosomes: integrating structure and function. Annu. Rev. Genet. **33:** 603–754.

Communicating editor: M. P. Colaiácovo